

## **COUPLED THERMAL-HYDRAULIC-MECHANICAL MODELLING OF THE CANISTER RETRIEVAL TEST**

**R. Guo**

Atomic Energy of Canada Limited, Chalk River Laboratories  
Chalk River, ON, Canada

**D. Dixon**

Atomic Energy of Canada Limited, Whiteshell Laboratories  
Pinawa, MB, Canada

### **ABSTRACT**

One of the in-situ tests chosen for examination as part of a series of numerical simulations undertaken for the Engineered Barriers Systems Task Force (EBS-TF) is the Canister Retrieval Test (CRT) carried out in the Äspö Hard Rock Laboratory. The CRT basically aims at demonstrating the practicality of recovering emplaced containers after the bentonite is fully saturated and has developed its maximum swelling pressure. The CRT also studies the thermal, hydraulic and mechanical evolution in the buffer from start until full water saturation. In the CRT, an electrically heated full-scale container is lowered into a deposition hole lined with cylindrical blocks and ring-shaped blocks of bentonite in the fall of 2000 and retrieved after five years of operation in early 2006. A large number of instruments measure pressure, temperature and other parameters during this time. Coupled thermal-hydraulic (TH) and coupled thermal-hydraulic-mechanical (THM) simulations for the CRT are conducted using the CODE\_BRIGHT program in order to evaluate the effectiveness of its modelling code in matching the observed evolution of the coupled processes in unsaturated bentonite material. The measured temperatures in the bentonite materials and in the rock are well simulated except for the measurements located in bentonite bricks because of the inadequate of thermal characterization of the bentonite bricks. The simulated liquid saturation profiles at the end of the test matched the measurements very well at different layers. The simulated vertical stresses in the bentonite materials capture the trends and the value of measurements reasonably well.

### **1. INTRODUCTION**

One option for the disposal of used nuclear fuel involves placement of used-fuel containers (referred to as canisters in the SKB and Posiva concepts) in boreholes excavated in the floor of repository tunnels located deep within a geologic medium.

One of the in-situ tests associated with development of the deep geological disposal concept in Sweden is the Canister Retrieval Test (CRT)<sup>1</sup>, carried out in the Äspö Hard Rock Laboratory. The Canister Retrieval Test is intended to demonstrate the retrievability of emplaced containers after the bentonite buffer (i.e., bentonite materials installed immediately adjacent to the container) is fully saturated and has developed its maximum swelling pressure. However, the test is also useful in studying the thermal, hydraulic and mechanical evolution in the buffer from start of emplacement until full water saturation. In the CRT, an electrically heated full-scale

---

<sup>1</sup> O. Kristensson, L. Börjesson. CRT-canister retrieval test: EBS task force assignment.

container is installed in a deposition hole lined with cylindrical blocks and ring-shaped blocks of bentonite. After over five years of operation the test is recovered early in 2006. A large number of instruments that measured pressure, temperature and other parameters are monitored throughout the test's operation, providing a record of the system's evolution. In order to evaluate the effectiveness of several mathematical models in evaluating the evolution of the coupled processes in unsaturated bentonite material, results from the CRT are shared among an international group of numerical modellers, the Engineering Barrier System Task Force (EBS-TF) modelling group in order to allow comparisons of modelling results to the physical measurements recorded. Atomic Energy of Canada Limited (AECL), representing the Nuclear Waste Management Organization, is a member of the EBS TF modelling group until 2011 and undertook modelling exercises on their behalf.

## 2. DESCRIPTION OF THE CANISTER RETRIEVAL TESTS

Schematic three-dimensional and plan views of the CRT are given in Figure 1. Figure 2 shows schematic layouts of the experiment, its dimensions and the locations of instruments, at which the measurements are compared with simulated results. The CRT is installed in a vertical borehole drilled in the bottom of a horizontal tunnel in granite in the Äspö Hard Rock Laboratory. The tunnel cross section at the location of the CRT has the approximate dimensions of 6-m x 6-m with a horseshoe profile. There are 16 filter mats of 10-cm-width installed uniformly around the perimeter of the borehole from 0.15 m from the bottom to 6.25 m height against the borehole wall. Below the container, there is a 0.5-m-thick bentonite cylindrical block (C1). Vertically 0.5-m-thick bentonite ring-shaped blocks with a radial thickness of 0.285 m (R1 through R10) are placed in the space between the container and the granite. A 10-mm-thick gap existed between the outer surface of the container and the inside surface of the bentonite ring-shaped blocks. The volume between the top surface of the container and the top surface of the upper most ring-shaped block (R10) is filled with about 220~230-m-thick bentonite bricks as shown in Figure 2. Three layers of 0.5-m-thick bentonite cylindrical blocks (C2, C3 and C4) are placed between the top surface of the bentonite bricks and the bottom of the retaining concrete

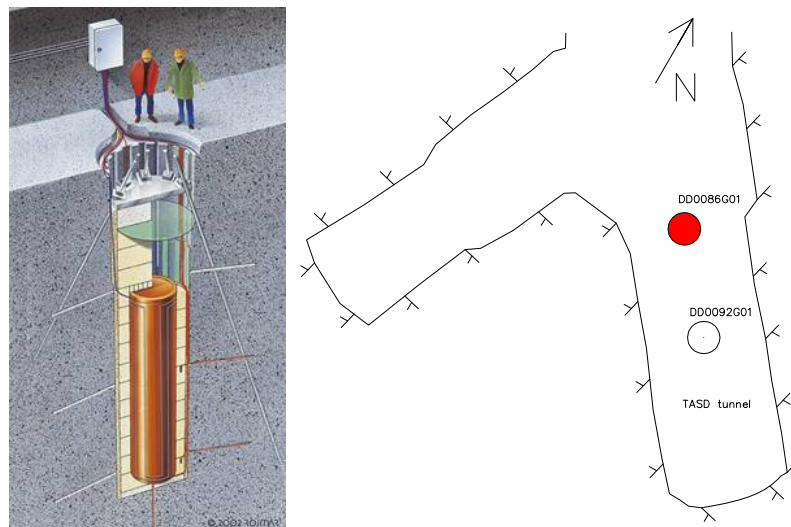


**Figure 1. Illustration of the experimental set-up of the CRT and the location in the TASD tunnel (Figures provided by SKB).**

plug. Bentonite pellets fill the gap between the bentonite blocks and the filter mats. An impermeable rubber seal is installed between the upmost bentonite block C4 and the bottom of the concrete plug, which is further capped by a steel lid. The concrete plug and the steel lid are restrained by nine inclined rock anchors.

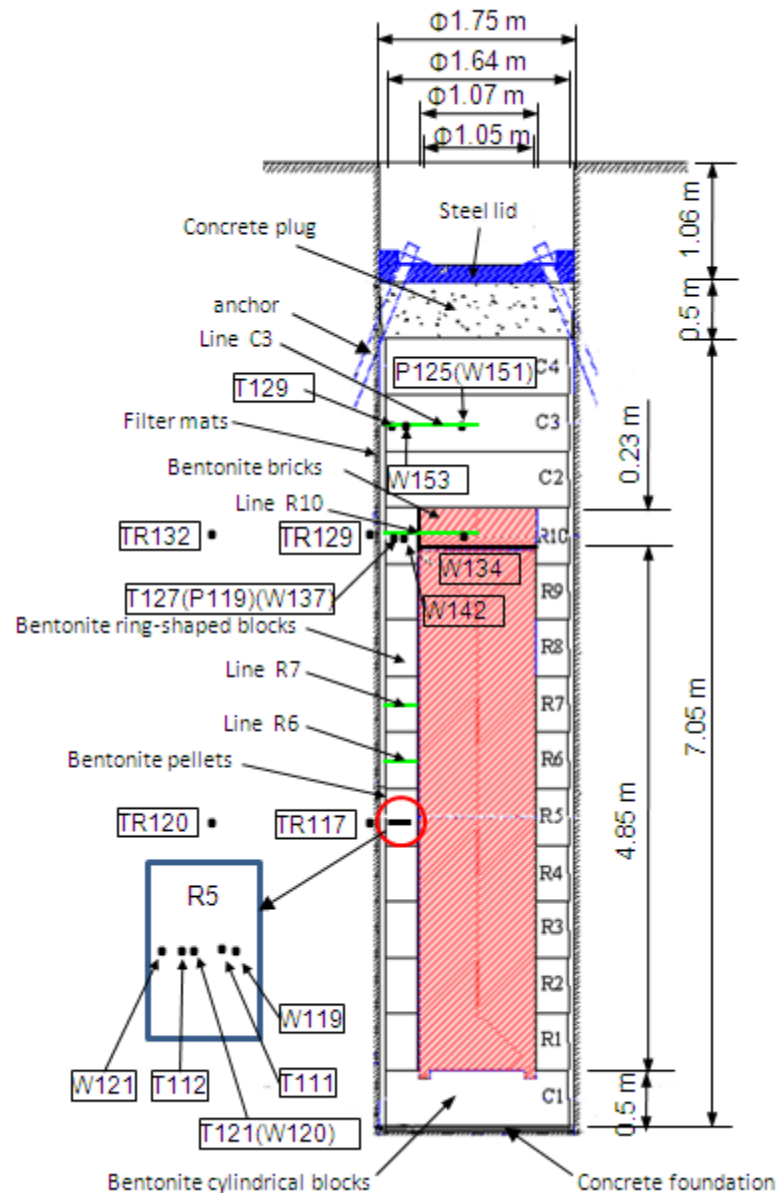


**Figure 2. Schematic vertical section of the CRT layout showing the locations of sensors, at which measurements were recorded.**

The detailed heater power protocol for the experiment is shown in Figure 3. Heating of the CRT is initiated with a constant power of 700 W on October 23, 2000 (day 1), one day after casting the concrete plug. Heating is maintained in successive periods with increased power of 1700 W (109 days) and 2600 W (574 days), and subsequent decreased power in later periods of 2100 W (450 days), 1600 W (462 days) and 1150 W (215 days).

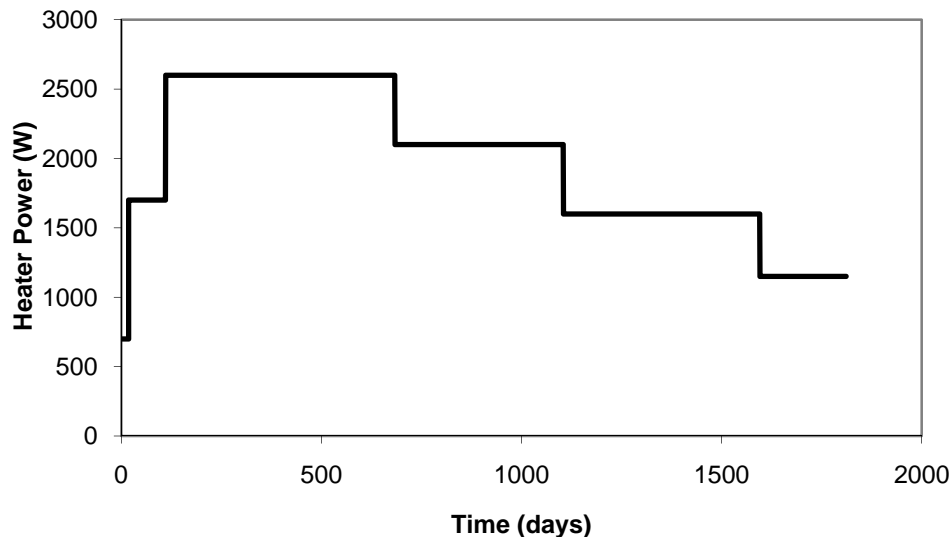


**Figure 3. Container power protocol of the CRT.**

The detailed water pressure protocol is shown in Figure 4. The water pressure in the filter mats is 0 kPa beyond simple static head at day 1 and then increases stepwise to 0.8 MPa in the period of September 5 to October 10, 2002 (days 687-713). The water pressure in the mats decreases abruptly to 0.1 MPa over a short period between day 770 and day 804, increases to 0.4 MPa between day 804 and day 819 and then increases again to 0.8 MPa between day 819 and day 1598 and finally decreases rapidly again to 0 kPa until the end of the test.

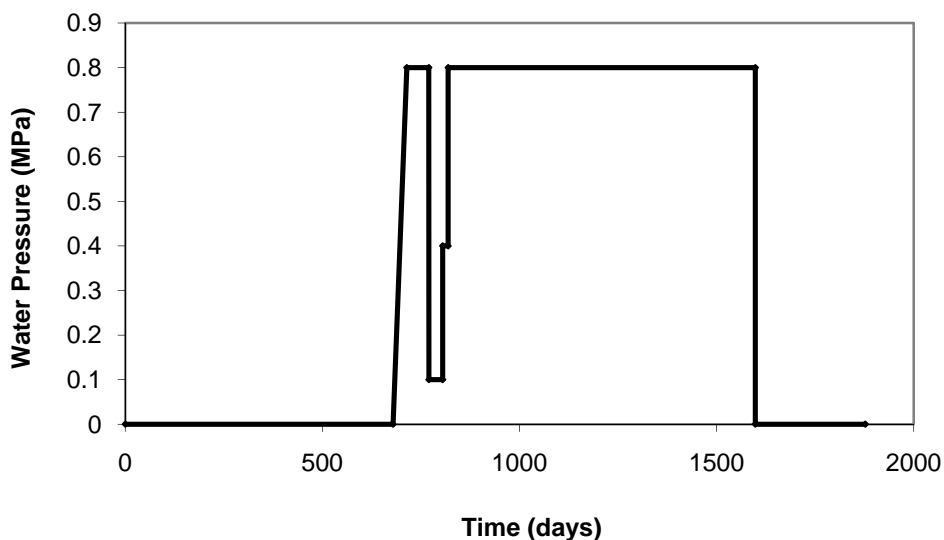


**Figure 4. Filter mat pressure protocol of the CRT.**

**Instrumentation:** The locations of some of the instruments installed in the bentonite ring-shaped blocks R5 and R10, bentonite cylindrical block C3 and in the bentonite bricks are shown in Figure 2. The Vaisala sensors (indicated with prefix “W”), which measure soil relative humidity (and hence water content), function very well for a 600-day period when the relative humidity is below 96%, but do not survive a sudden temperature drop at 600 days. Pressure sensors (shown by prefix “P”) are used to measure the vertical total pressures in the bentonite rings and cylinders. Temperature sensors (indicated by prefix “T”) function reliably for the entire duration of the CRT.

### 3. DESCRIPTION OF THE CODE\_BRIGHT PROGRAM

Coupled thermal-hydraulic (TH) and thermal-hydraulic-mechanical (THM) simulations of the CRT are performed using CODE\_BRIGHT, a general-purpose finite element program for the analysis of coupled THM phenomena in geological media and developed by Universidad Politècnica de Catalunya [1]. This program has been extensively used in international benchmark exercises and has been applied to the analysis of different geoenvironmental projects, waste disposal and geotechnical problems involving saturated/unsaturated soil behavior [2], [3], [4].

The THM version of CODE\_BRIGHT program solves the main governing equations, which describe heat transfer, moisture migration, solute transport and air transfer in the material, coupled with stress/strain behavior. Detailed presentation of the governing equations for coupled THM analysis considered in this paper can be found in [2], [5] and [6]. However, a brief description of the Barcelona Basic Model, which is used as the mechanical constitutive model of the bentonite is presented here for introduction of related material parameters.

The Barcelona Basic Model, an elasto-plastic model [7], is used to simulate the behaviour of the bentonite buffer. In order to help understand the selection of parameters, some of the mechanical equations used in this modelling are presented in the following section.

The volumetric elastic strain ( $d\varepsilon_v^e$ ) can be calculated using the following equation:

$$d\varepsilon_v^e = \frac{k}{1+e} \frac{dp'}{p'} + \frac{k_s}{1+e} \frac{ds}{s+a_0} + \alpha_0 dT \quad (1)$$

where  $p'$  is the mean effective stress and is equal to  $\frac{1}{3}(\sigma_x + \sigma_y + \sigma_z) - \max(p_g, p_l)$ ;

$p_g$  is the pore gas pressure;

$p_l$  is the pore liquid pressure;

$k_s$  is a compressibility coefficient for strain in response to changes in suction ( $s$ );

$k$  is a compressibility coefficient for the response to mean stress changes;

$a_0$  is the atmospheric pressure;

$\alpha_0$  is the volumetric thermal expansion; and

$T$  is the temperatures.

The plastic strain can be obtained by plastic theory. The equations for the yield curve in  $(p', s)$  space is:

$$\left(\frac{p_0}{p^c}\right) = \left(\frac{p_0^*}{p^c}\right)^{[\lambda(0)-k]/[\lambda(s)-k]} \quad (2)$$

where  $p_0$  is preconsolidation stress at varying suction ( $s$ );

$p_0^*$  is preconsolidation stress for saturated conditions;

$p^c$  is a reference stress; and

$\lambda(s)$  is the stiffness parameter at a given suction ( $s$ ).

$\lambda(s)$  is calculated by:

$$\lambda(s) = \lambda(0)[(1-r)\exp(-\xi \cdot s) + r] \quad (3)$$

where  $\lambda(0)$  is the stiffness parameter at saturation;

$r$  is a parameter defining the maximum soil stiffness;

$s$  is suction; and

$\xi$  is a constant describing the rate of increase in soil stiffness with suction.

## 4. GEOMETRY, BOUNDARY CONDITIONS AND INITIAL CONDITIONS

### 4.1 Geometry

Figure 5 shows the geometry and the dimensions of the axisymmetrical 2-D model. The radial dimension is 60 m from the axis of the borehole to the outer surface of the model. The distance from the top of the model to the roof of the tunnel is 50 m and the distance from the bottom of the model to the bottom of the borehole is also 50 m. The two-dimensional model includes 9 components, i.e. host rock, heater, bentonite pellets, bentonite bricks, bentonite ring-shaped blocks, bentonite cylindrical blocks, empty peripheral gap, concrete plug and steel lid.

### 4.2 Boundary conditions and initial conditions

#### 4.2.1 Boundary conditions

*Thermal Boundary Conditions:*

- The temperatures at the nodes on the tunnel surface and on the top of steel lid are set at 15°C.
- There is no heat flux at the nodes on the top, the axis of the model, the bottom and the outer vertical boundary of the model.
- The heat flux is uniformly applied at the nodes of the container and the total heat flux is equal to the power protocols of the CRT as shown in Figure 3.

*Hydraulic Boundary Conditions:*

- There is no water flux on the top, the bottom and the outer vertical boundaries of the model, along the axis of the model, nor on the tunnel surface and the top surface of steel lid.
- The hydraulic head at the nodes of bentonite pellets is fixed at the water pressure from filter pressure protocol as shown in Figure 4.

*Mechanical Boundary Conditions:*

- The nodes of the granite are vertically and horizontally fixed; and
- The nodes of the container heater are vertically and horizontally fixed.

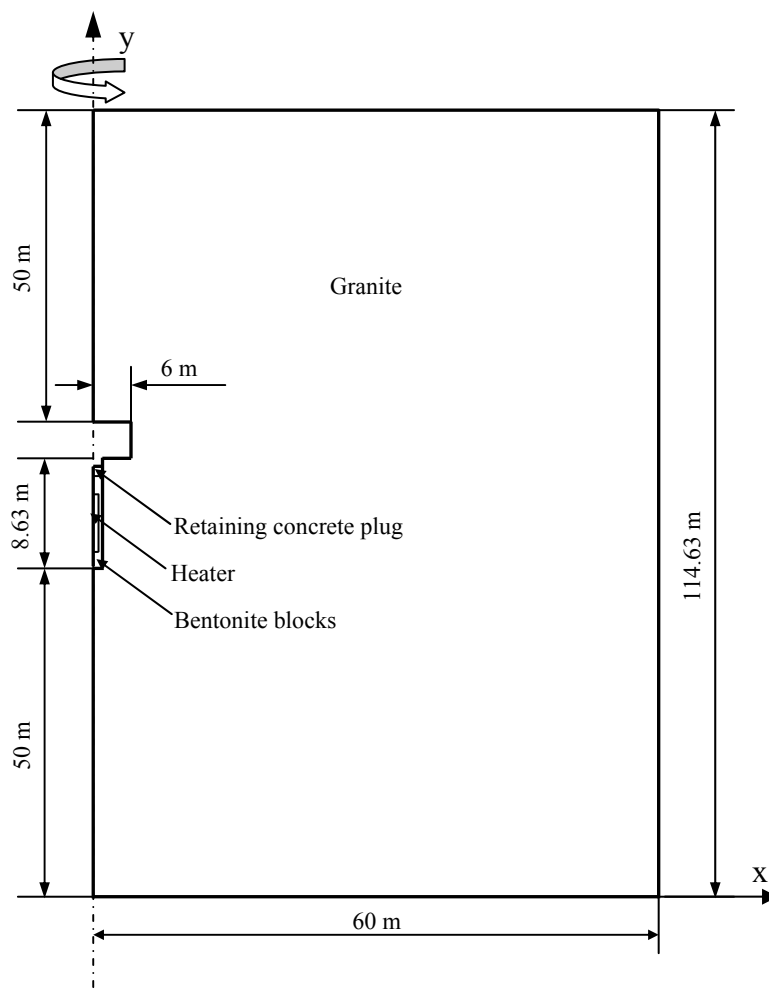


**Figure 5. Dimensions of the two-dimensional model.**

#### 4.2.2 Initial conditions

*Initial thermal Conditions:*

- Initial temperatures on all nodes are set at 20°C.

*Initial Hydraulic Conditions:*

- Initial saturations of bentonite cylinder-shaped blocks, bentonite ring-shaped blocks, bentonite pellets and bentonite bricks are set at 0.751, 0.859, 0.895 and 0.627, respectively.
- Initial saturation of gap is set at 1.0.
- Initial saturation of other materials is set at 0.

*Initial Mechanical Conditions:*

- Initial displacements in the X- and Y- directions for all of nodes in the model are set at 0.
- Initial stresses are equally set at 0.5 MPa in the X- and Y-directions.

**4.3 Material parameters****4.3.1 Hydraulic parameters of materials***Bentonite materials*

The initial degree of saturation, the dry density, void ratio and the specific gravity for the bentonite cylindrical blocks, bentonite ring-shaped blocks, bentonite bricks and bentonite pellets are shown in Table 1.

The relation between saturation and suction for the bentonite materials using the CODE\_BRIGHT manual suggested equation is as follows:

$$S_{re} = \left[ 1 + \left( \frac{S}{P_0} \right)^{1/(1-\beta_1)} \right]^{-\beta_1} \quad (4)$$

where  $s$  is suction, MPa;  $P_0$  is an estimated parameter;  $\beta_1$  is an estimated parameter. Based on the measurements in [9], [10] and [11], the values of  $P_0$  and  $\beta_1$  for the bentonite cylindrical blocks, the bentonite ring-shaped blocks, the bentonite bricks, and the bentonite pellets are shown in Table 1.  $S_{re}$  is the effective degree of saturation.  $S_{re}$  is expressed as follows:

$$S_{re} = \frac{S_r - S_{rres}}{S_{rmax} - S_{rres}} \quad (5)$$

where  $S_r$  is the absolute degree of saturation,  $S_{rres}$  is the degree of residual saturation (i.e., 0.05) and  $S_{rmax}$  is the degree of maximum saturation (i.e., 1.0).

The values of the saturated hydraulic conductivity for the bentonite cylindrical blocks, ring-shaped blocks, bricks and pellets are shown in Table 1. The relative permeability of the liquid phase ( $k_{rl} = S_{re}^4$ ) is adopted for all of bentonite materials. Relative permeability is the ratio of the permeability at a certain degree of saturation to the permeability at maximum saturation.

The hydraulic parameters of bentonite ring-shaped blocks are also used as the responding parameters for the empty gap.

**Table 1. Thermal and hydraulic parameters of bentonite materials.**

parameters	cylindrical	Ring-shaped	bricks	pellets
Initial saturation [8]	0.751	0.849	0.637	0.895
Dry density (kg/m <sup>3</sup> ) [8]	1699	1782	1616	1001
Void ratio [8]	0.636	0.56	0.72	1.778
Specific gravity [8]	2.65	2.65	2.65	2.65
Retention curve P <sub>0</sub> (MPa)	40	40	40	10
Retention curve, β	0.4	0.4	0.4	0.6
Thermal conductivity (W/(m·K))	λ <sub>max</sub> = 1.3 λ <sub>min</sub> = 0.3	λ <sub>max</sub> = 1.3 λ <sub>min</sub> = 0.3	λ <sub>max</sub> = 1.3 λ <sub>min</sub> = 0.3	λ <sub>max</sub> = 1.3 λ <sub>min</sub> = 0.17
Saturated hydraulic conductivity (m/s) [12]	k <sub>sat</sub> = 2.1x10 <sup>-14</sup>	k <sub>sat</sub> = 0.8x10 <sup>-14</sup>	k <sub>sat</sub> = 0.8x10 <sup>-14</sup>	k <sub>sat</sub> = 0.8x10 <sup>-11</sup>

#### *Rock, steel, concrete and heater*

*The host rock, steel shell, concrete plug and heater are treated as impermeable and are assigned a 6 orders of magnitude lower hydraulic conductivity than the bentonite and a retention curve using Equation (4) with  $P_0=1 \times 10^{-6}$  and  $\beta_1 = 0.5$ .*

#### 4.3.2 Thermal Parameters of Materials

The following expression of the variation of bentonite thermal conductivity with saturation is used in this calculation.

$$\lambda = \lambda_{sat}^{S_i} \lambda_{dry}^{(1-S_i)} \quad (6)$$

in which  $\lambda_{sat}$  is the saturated thermal conductivity of the bentonite and  $\lambda_{dry}$  is the dry thermal conductivity of the bentonite. Based on the measured information in [13], the values of  $\lambda_{sat}$  and  $\lambda_{dry}$  for bentonite cylindrical blocks, ring-shaped blocks, bricks and pellets are shown in Table 1. The specific heat of the bentonite materials is set at 800 J/(kg·K).

The thermal conductivity of the host rock, the steel shell, the concrete plug and heater are set to 2.51 W/(m·K), 50 W/(m·K), 2.7 W/(m·K) and 300 W/(m·K), respectively. The specific heats of these mediums are set at 770 J/(kg·K), 460 J/(kg·K), 770 J/(kg·K) and 460 J/(kg·K), respectively. The thermal parameters of ring-shaped blocks are also using as the thermal parameters for empty gap.

#### 4.3.3 Mechanical Parameters of Materials

The cylindrical bentonite blocks, the ring-shaped bentonite blocks and bentonite bricks are assumed to be elasto-plastic materials. The mechanical parameters for the bentonite blocks and

bricks are shown in Table 2. The concrete plug, steel lid, bentonite pellets and empty gap are assumed to be linear elastic materials. Their mechanical parameters are shown in Table 3.

**Table 2. Mechanical parameters used for bentonite materials (blocks and bricks) in the coupled THM modeling.**

	<b>Cylindrical bentonite blocks</b>	<b>Ring-shaped bentonite blocks</b>	<b>Bentonite bricks</b>
$P_0^*$ (MPa)	0.359	0.359	0.359
$\chi(0)$	0.621	0.621	0.621
$\kappa$	0.28	0.28	0.28
$r$	0.75	0.75	0.75
$\beta$ (MPa <sup>-1</sup> )	0.05	0.05	0.05
$p^c$ (MPa)	0.18	0.18	0.18
$k_s$	0.04	0.04	0.04
$\nu$	0.2	0.2	0.2
$G$ (MPa)	24	24	24
$M$	0.526	0.526	0.526
$\alpha_0$ (°C <sup>-1</sup> )	$3 \times 10^{-5}$	$3 \times 10^{-5}$	$3 \times 10^{-5}$

**Table 3. Mechanical parameters used for concrete plug, steel lid, bentonite pellets and empty gap**

	<b>Concrete plug</b>	<b>Steel lid</b>	<b>Bentonite pellets</b>	<b>Empty gap</b>
Young's modulus, $E$ , (MPa)	30,000	200,000	3	3
Poisson's ratio, $\nu$	0.2	0.2	0.2	0.2
Linear thermal expansion, $\alpha$ , (°C <sup>-1</sup> )	$9.8 \times 10^{-5}$	$1.6 \times 10^{-5}$	$1 \times 10^{-5}$	0

## 5. MODELLING RESULTS AND COMPARISON WITH MEASUREMENTS

### 5.1 Thermal response

#### 5.1.1 Bentonite materials

Figure 6 shows the comparison of the simulated temperatures with measurement at three different locations on layer R5 (see Figure 2). The simulated temperatures match the measurements reasonably well at these locations for the first 900 days of CRT operation. After 900 days, the simulated temperatures are consistently about 2~4°C lower than the measurements. The likely reason for this divergence is the influence of the nearby Temperature Buffer Test (TBT) which is not considered in the numerical simulation. The TBT is another borehole-buffer-heater test at very high temperatures at a distance of only 6 m distance from the CRT, which results in relatively higher temperatures developing within the CRT.

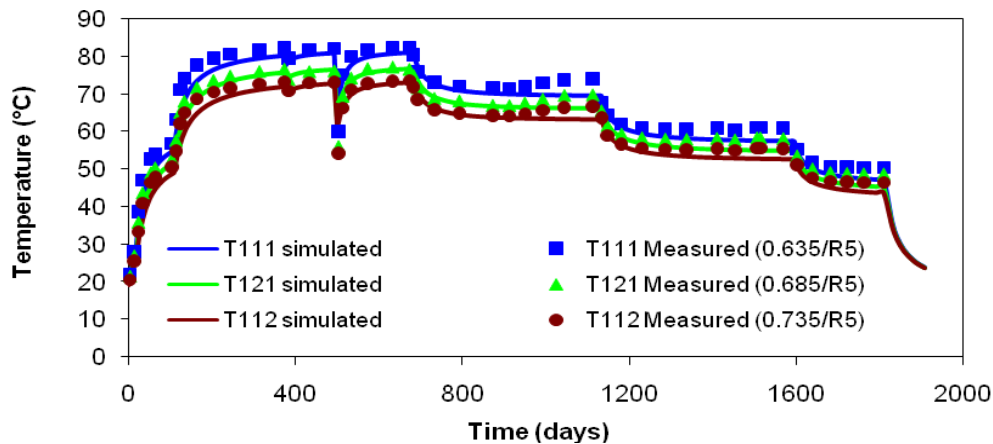


**Figure 6. Comparison of temperatures between simulated results from 2-D model and measurements at sensors of three sensors in the buffer component of the CRT.**

Figure 7 shows the comparison of the simulated temperatures and recorded measurements at locations of sensors T127 and T129 (see Figure 2). The simulated temperatures at T127 in layer R10 are about 8°C higher than actual measurements, which is attributed to uncertainties related to the hydraulic parameter used for the bentonite bricks. The simulated temperatures at T129 in layer C3 match the measurement reasonably well up to around day 900 of the experiment, after which, the nearby TBT influences the near-field thermal conditions in the CRT (resulting in higher recorded temperatures).

#### 5.1.2 Host rock

Figure 8 shows the comparison of the simulated temperatures with measurements at several sensor locations in the host rock surrounding the CRT (see Figure 2). Sensors TR117 and TR120 are situated respectively adjacent to and more distant from the container along layer R5 of the experiment. Sensors TR129 and TR132 are similarly situated adjacent to and more distant from the container, respectively, along layer R10. All of the simulated temperatures match the field measurements very well, indicating that the parameters used for the rock are reasonable.

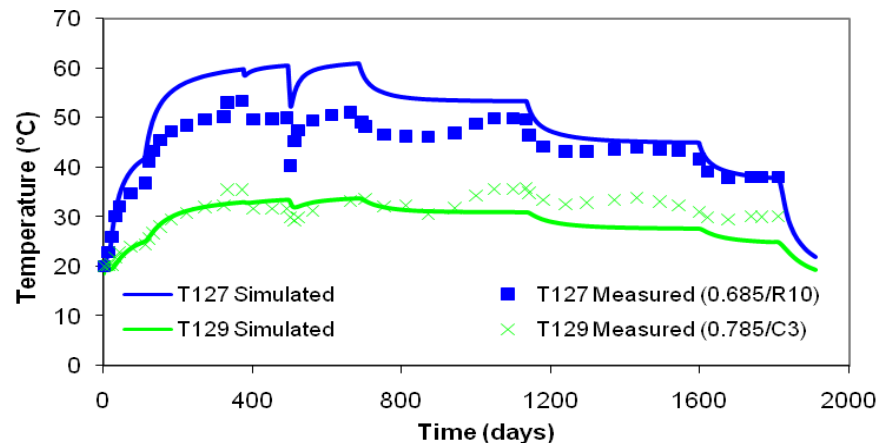


**Figure 7. Comparison of the simulated and measured temperatures at sensor locations T127 (in R10) and T129 (in C3) of the buffer component of the CRT**

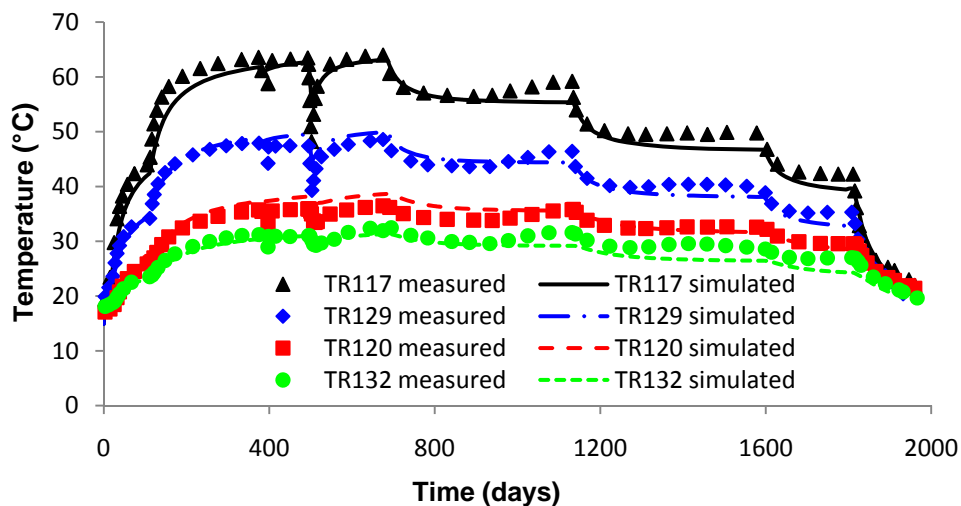
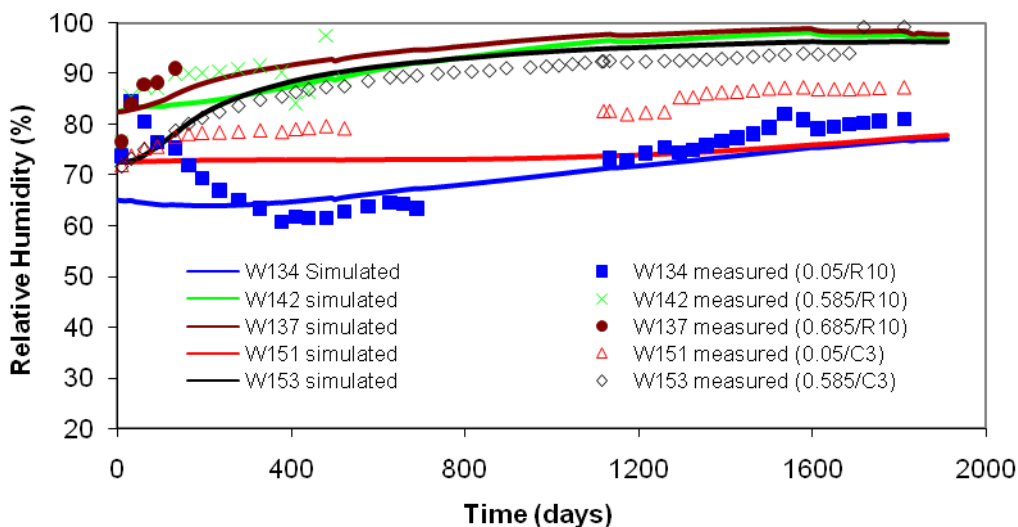


**Figure 8. Comparison of simulated temperatures with measurements at four locations in the host rock surrounding the CRT**

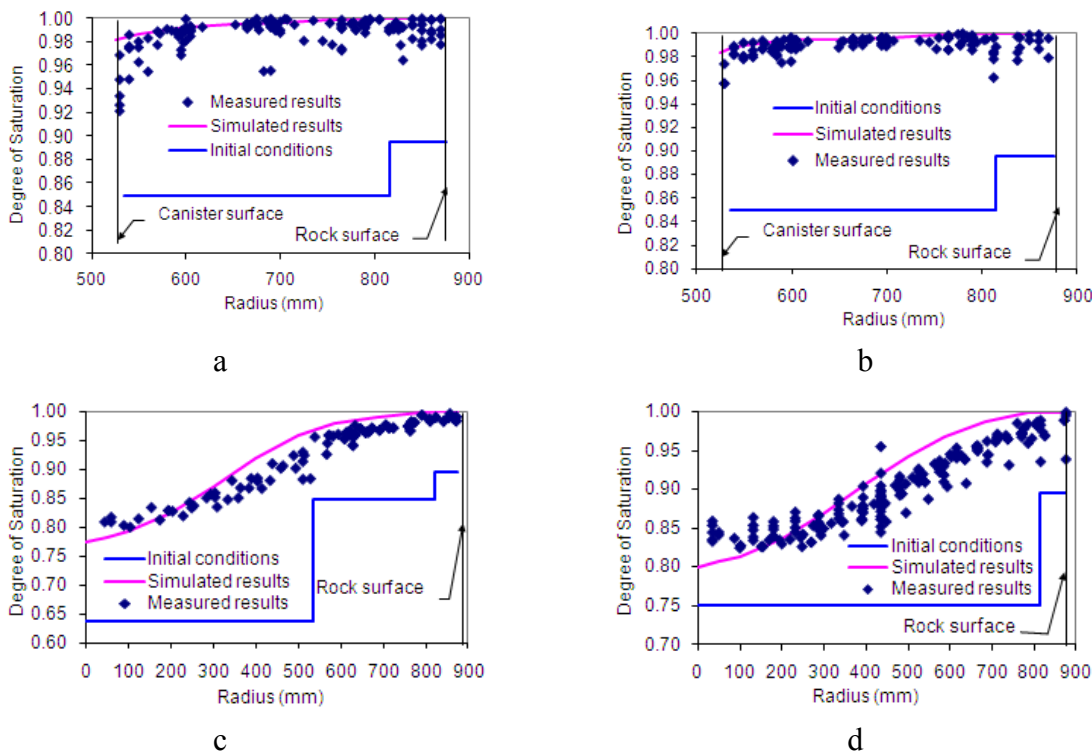
## 5.2 Comparison of hydraulic response between simulated results and measurements

Figure 9 shows the comparison of simulated relative humidity with field measurements for five locations (sensors W134, W142 and W137 in layer R10 and sensors W151 and W153 in layer C3) (see Figure 2). The simulated results provide a good match to the recorded data, with the exception of those for W151 in layer C3, where for undetermined reasons the model under-predicts humidity.

Figure 10 shows the comparison of simulated water saturation profiles with measurements along lines in layers R6, R7, R10 and C3 at the end of the test (see Figure 2). The simulated water saturation profiles capture the general trends provided by the sensor measurements.



**Figure 9. Comparisons of simulated relative humidity with measurements in layers C3 and R10.**



**Figure 10. Comparison of water saturation simulations with measured results along (a) Line R6, (b) Line R7, (c) Line R10 and (d) Line C3 of the bentonite in the CRT.**

Figure 11 shows the comparison of the simulated relative humidity with field measurements for the sensor locations W119, W120 and W121 at layer R5 (see Figure 2). Since these sensors fail

within 600 days of operation, no direct data are available for the following period. The simulated relative humidity for W121 matches the measurement very well. The simulated relative humidity for W119 and W120 is lower than the measured results.

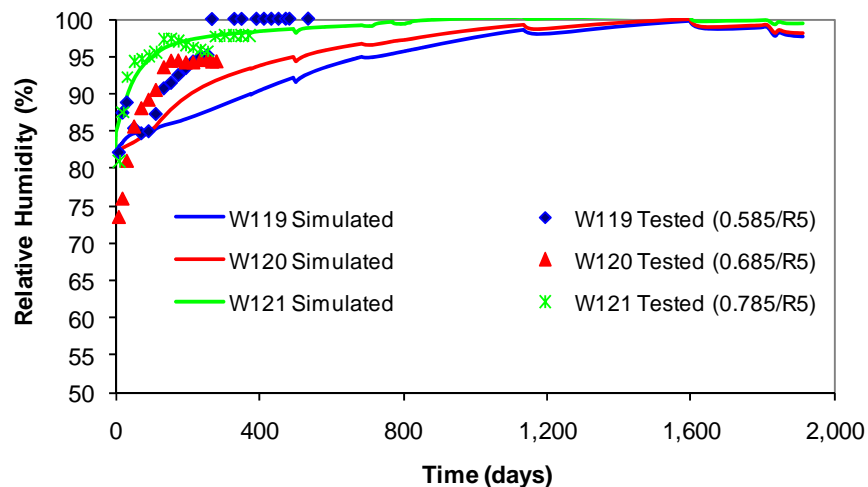


**Figure 11. Comparison of the simulated relative humidity with field measurements (during the first 600 days) and predicted relative humidity (after 600 days) at sensor locations W119, W120 and W121.**

### 5.3 Mechanical response

During coupled THM modelling, a convergence problem is encountered when the simulation reaches 684 days after the start of the experiment. This is caused by the application of the boundary hydraulic pressure increase conditions, which might cause a greater tensile stress in the bentonite materials. The convergence problem has not been resolved in this paper.

Figure 12 shows the comparison of the simulated vertical stresses and measured results at sensor locations of P119 in layer R10 and P125 in layer C3. The simulation captures the general trends observed in the field measurements.

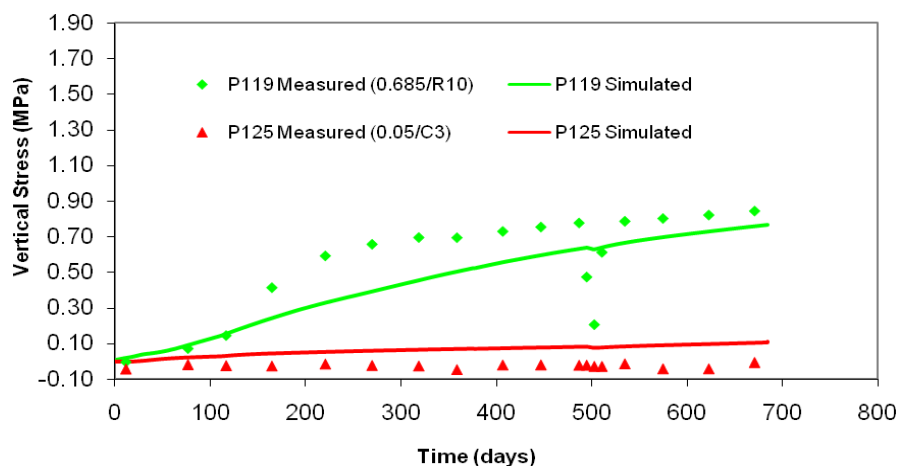


**Figure 12. Comparison of the simulated vertical stresses and measured results at sensor locations P119 and P125.**

## 6. SUMMARY

Coupled TH and coupled THM simulations for the CRT are completed using CODE\_BRIGHT. In this modelling activity, the results can be summarized as follows.

- In two regions occupied by the bentonite blocks (R5 and C3), the temperatures predicted by the numerical simulation match the measurements well.
- In a third region occupied by bentonite bricks (R10), the simulated temperatures are 8°C higher than the measurements during the first 900 days. This is attributed to a combination of inadequate thermal characterization of the bentonite bricks and thermal interference by the nearby TBT. After 900 days the simulation matches the field measurements more closely.
- In the host rock, the simulated temperatures match the measurements very well at all locations considered.
- In blocks R5, R10 and C3, the numerical simulations of relative humidity capture the trends and magnitude of the observed conditions. Only data from one sensor (W153) fail to be replicated in the numerical simulations and it is uncertain if this is sensor-related or code-related.
- The simulated liquid saturation profiles match the measurements very well at different layers (R6, R7, R10 and C3) at the end of tests.

The simulated vertical stresses at layers R10 and C3 match the trends and magnitudes recorded by the sensor measurements.

## ACKNOWLEDGEMENTS

The modeling work described in this paper was supported by the Nuclear Waste Management Organization (NWMO) as part of their contributions to the Engineered Barriers System Task Force. The author also thanks Clay Technology AB of Sweden for supplying to the members of the EBS TF, the data from the CRT experiment and the materials properties values used in the this work. Contributions to this paper by AECL technical reviewers is also appreciated.

## REFERENCES

- [1] Olivella, S., Gens, A., Carrera, J., Alonso, E.E. "Numerical modelling for a simulator (CODE\_BRIGHT) for the coupled analysis of saline media". *Engineering Computations* 13(7): 1996. 87-112.
- [2] Gens, A., Garcia-Molina, A.J., Olivella, S., Alonso, E.E., Huertas, F. "Analysis of a full scale in situ test simulating repository conditions". *Int. J. Numer. Anal. Mech. Geomech.* 22, 1998, pp. 515-548.
- [3] Gens, A., Sánchez, M., Guimaraes, L., Alonso, E., Eloret, A., Olivella, S., Villar, M., Huertas, F. "A full-scale in situ heating test for high-level nuclear waste disposal: observations, analysis and interpretation". *Geotechnique* 59 (4): 2009. 377-399.
- [4] Hökmark, H., Ledesma, A., Lassabatere, T., Fälth, B., Börgesson, L., Robinet, J.C., Sellali, N., Sémété, P. "Modelling heat and moisture transport in the ANDRA/SKB temperature buffer test". *Physics and Chemistry of the Earth* 32: 2007. 753-766.
- [5] Olivella, S., Carrera, J., Gens, A., Alonso, E. E. "Nonisothermal multiphase flow of brine and gas through saline media". *Transport Porous Media* 15: 1994. 271-293.

- [6] Rutqvist, J., Börgesson, L., Chijimatsu, M., Kobayashi, A., Jing, L., Nguyen, T. S., Noorishad, J., Tsang, C. –F. “Thermohydromechanics of partially saturated geological media: governing equations and formulation of four finite element models”. *International Journal of Rock Mechanics and Mining Sciences* 38, 2001. 105-127.
- [7] Alonso, E.E., Gens, A., Josa, A. “A constitutive model for partially saturated soils”. *Geotechnique* 40, 1990. pp. 405-430.
- [8] Gatabin C. Billaud, P. “Bentonite THM mock-up experiments sensors data report”. CEA, NT DPC/SCCME 05-300-A. 2005.
- [9] Hökmart, H., Falth, B. “Temperature buffer test. Predictive modelling programme”. Äspö Hard Rock Laboratory Internal Report F12.1G 1012125. 2003.
- [10] Dang, K.D., Robinet, J.-C. “Thermo-hydro-mechanical behaviour of MX80 bentonite for temperature  $\geq 100^{\circ}\text{C}$ ”. Final Report, ANDRA Report C.RP.0EUG.02.008. 2004.
- [11] Villar M.V. AESOIE Hard rock laboratory. CIEMAT contribution to 2001 Annual Scientific Report. CIEMAT Internal Report CIEMAT/DIAE/54540/2/03. 2003.
- [12] Börgesson, L., Hernelind, J. “Preliminary modelling of the water-saturation phase of the buffer and backfill materials”. Äspö Hard Rock Laboratory. SKB IPR-00-11. 1999.
- [13] Börgesson, L., Johannesson, L.-E., Sandén, T., Hernelind, J. “Modelling of the physical behaviour of water saturated clay barriers. Laboratory tests, material models and finite element application”. SKB Technical Report 95-20. 1995.